X-Band Opacity of a Tropical Tree Canopy and its Relation to Intercepted Rain, Eddy Fluxes and other Meteorological Variables

Marc Schneebeli
and Christian Mätzler
Institute of Applied Physics
University of Bern
Bern, Switzerland
Email: schnee@iap.unibe.ch

Sebastian Wolf
and Werner Eugster
Institute of Plant Sciences
Federal Institute of Technology
Zurich, Switzerland
Email: sebastian.wolf@ipw.agrl.ethz.ch

***Abstract*—During Summer and Autumn 2007, we deployed a 11 GHz microwave radiometer in an experimental tree plantation in Sardinilla, Panama, in the vicinity of the Panama Canal. With this instrument, we determined the opacity of the tree canopy. A collocated eddy-covariance flux tower measured water vapor and carbon dioxide fluxes as well as other meteorological variables such as photosynthetically active radiation (PAR), vapor pressure deficit (VPD) and rain. We observed a pronounced diurnal cycle of the opacity during dry periods and a close relation of the opacity to canopy intercepted rain during rainy periods. The diurnal opacity cycle shows a strong correlation with PAR, VPD and the water vapor flux.**

I. Introduction

Tropical rain forests play a dominant role in the earth's water cycle. Direct evaporation of rain and evapotranspiration are major sources of lower tropospheric humidity. A promising tool to monitor these processes is microwave radiometry.

Microwave properties of tree canopies have been investigated for many years and a good overview over this research topic is given in [1]. In contrast to the wealth of available information, reports on measurements of diurnal variations in tree opacities as well as observations of tree opacities focusing on intercepted water are rather sparse. In [2] the authors reported diurnal variations in the dielectric constant of the xylem and hypothesize a relation to the ascent of sap in the xylem. In [3] diurnal changes of the radar backscatter of tropical trees with the Ku-Band Radar of the TRMM satellite were studied and it was concluded that the signal has a relation to dew deposition. A large experiment on diurnal changes in the optical and microwave frequency range was reported in [4], although not very clear conclusions on diurnal behaviour could be drawn from their X-Band measurements. The measurement of the attenuation of a 10 GHz signal over a horizontal path through a Douglas fir stand was reported in [5] and a nice linear relation to intercepted rain was found. The authors then proposed this attenuation method as a tool to monitor rain water interception.

978-1-4244-1987-6/08/$25.00 © 2008 IEEE

Recently, because of the launch of the SMOS satellite in the near future, L-Band attenuation through tree canopies becomes more and more interesting and therefore several studies are being performed with L-Band radiometers. A very recent study measured the L-Band and X-Band transmissivities of a deciduous forest site during 4 months with a method similar to ours but the focus of this work was not put on diurnal changes [6].

In our experiment to be presented here, we measured the brightness temperature of a tropical tree canopy, consisting of *Anacardium excelsum*, *Tabebuia rosea* and *Hura crepitans*. These trees are part of an experimental biodiversity plantation, have an age of about seven years and an average height of 8 m. We modeled the incoming sky radiation with a radiative transfer model which allowed us to calculate the canopy opacity. We accounted for the effect of temperature on the opacity with a simple canopy opacity model. Finally we state that the difference between the opacity model and the measured opacity originates from unaccounted dielectric changes in the tree, probably induced by sap flow, dew deposition and intercepted rain.

II. Experimental setup

Our microwave radiometer was placed on the ground, looking upwards through the canopy under an elevation angle of $40°$, measuring in horizontal polarization. The radiometer was placed below a tarp, which allowed us also to measure during rain. Data were gathered from July to October 2007. Figure 1 shows the instrument as it was deployed in the field.

A. Microwave radiometer

For this experiment, a simple single polarization 11.4 GHz microwave radiometer has been developed. For our purpose and in order to be deployed in a tropical environment, the instrument had to fulfill several requirements. First of all, we required an instrument with automated internal calibration, since tipping-calibration is not possible below the canopy and manual calibration with hot/cold loads not desirable. To

Fig. 1. The radiometer deployed in the field

achieve this, the instrument was equipped with a waveguide switch, switching every $5\,\mathrm{s}$ to an ambient load (internal termination load enclosed in a copper block). Every minute, additional $80\,\mathrm{K}$ noise from a solid state noise source was coupled in over a 20 dB cross coupler.

Second, the instrument required protection against tropical heat, high relative humidity, rain and insects. This was achieved with installing the radiometer together with the horn antenna in a sealed solid aluminum box. The radiation entered through a microwave transparent Styrofoam window in the box. The Schottky diode detectors and the noise source, being the most temperature critical components, were enclosed in a solid aluminum block and attached to a Peltier element, capable of heating and cooling. The temperature of this block was stabilized to 26° C such that the Peltier element had to cool during the day and to heat during the night, when we had high relative humidity.

Finally our system had built-in data acquisition and storage and was capable of unattended operation over several days. Data were taken every $100\,\mathrm{ms}$ and averaged over one full calibration cycle, which took $1\,\mathrm{min}$.

The radiometer has two channels, both measuring at the same center frequency but one with 50 MHz and the other with 500 MHz bandwith. The antenna we used is a rectangular horn with a beamwidth of about 15°. In addition to the microwave part, we installed a thermal infrared radiometer (Everest 4000.5 GL) into the box. A schematic drawing of the instrument can be found in Figure 2.

B. Other measurements

Collocated to the microwave radiometer, an eddy-covariance flux tower measured CO_2 and water vapor fluxes over the canopy. In addition, other variables like temperature, soil moisture, wind, photosynthetically active radiation (PAR) and relative humidity were also measured. Rain measurements were performed with two tipping buckets, of which one was placed below the canopy and another in the open field. The leaf area index (LAI) of the canopy was determined with hemispherical photography and the software 'Gap Light Analyzer' (© Simon Fraser University, Institute of Ecosystem Studies, BC).

III. Method and Measurements

A. Canopy opacity measurement

According to [7], the canopy transmissivity t_c can be expressed with the following equation:

$$t_c = \frac{T_c - T_{b,in}}{T_c - T_{b,\mathrm{sky}}} \tag{1}$$

T_c is hereby the physical canopy temperature measured with our infrared radiometer, $T_{b,in}$ is the brightness temperature measured with the microwave radiometer and $T_{b,\mathrm{sky}}$ is the brightness temperature emitted from the sky. This formula is valid if the emissivity of the ground is high and if the temperature difference between the ground and the canopy as well as the canopy reflectivity are low. The opacity is then calculated with the Beer-Lambert law, yielding the expression $\tau = -\log(t)$. What we can not measure with our configuration is the sky radiation $T_{b,\mathrm{sky}}$, and therefore this contribution needs to be modeled. To do so, we used ECMWF profiles of water vapor volume mixing ratio, pressure and temperature. Those profiles were interpolated on a quarter hour time grid and scaled with the measured ground values. Cloud water was added to the profile with an algorithm described in [8]. With the so derived atmospheric profiles, we calculated absorption coefficients with an atmospheric propagation model [9]. Radiative transfer calculations led then to the T_{b1} under rain free conditions, with typical values of $20\,\mathrm{K}$ at an elevation angle of 40°. In order to account for the rain contribution on the incoming sky radiation, we measured the sky brightness temperature during rain events and set the measured increase in brightness temperature in relation to the rain rate. We were then able to account for the rain contribution on the incoming sky radiation. It is clear that we cannot calculate the brightness temperature T_{b1} very accurately with the described technique, but the impact of T_{b1} on the canopy opacity is rather weak. An underestimation of T_{b1} of $20\,\mathrm{K}$ results in an opacity error of about 4%.

B. Canopy opacity model

For the interpretation of our measurements we incorporate an effective medium canopy opacity model of leaves, that treats scattering with a geometrical optics approach. It is described in [10] and reads:

$$\tau_c = A_p \cdot \mathrm{LAI} \cdot k d \epsilon'' \frac{1}{\cos\theta} t_l \tag{2}$$

with A_p being a geometrical factor we set to 1, the leaf area index LAI with a value of 3.5, the wave number k, leaf thickness d, the complex part of the leaf dielectric constant ϵ'', observaton angle θ and the single leaf transmissivity t_l. t_l can be computed with the coherent model for layered media, discussed for example in [11]. As input parameters the model requires the frequency, incidence angle, leaf thickness and

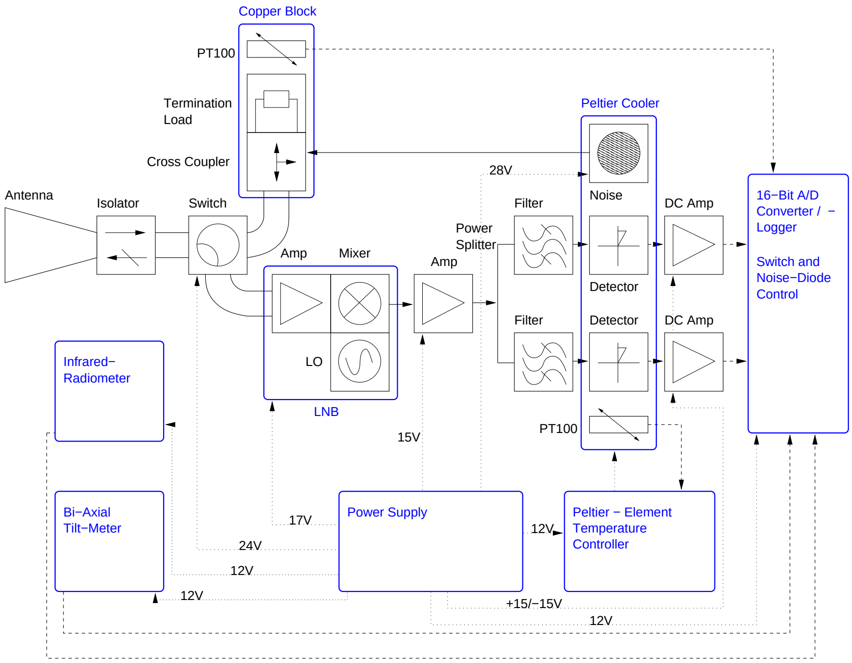

Fig. 2. Schematic drawing of the microwave radiometer

leaf dielectric constant ϵ. The leaf thickness distribution was measured and a mean value of approx. $0.2\,\mathrm{mm}$ was found. We determined the leaf dielectric constant with the semi-empirical model developed in [12]. It reads:

$$\epsilon = 0.522\,(1 - 1.32 m_d)\,\epsilon_{sw} + 0.51 + 3.84 m_d \qquad (3)$$

with the leaf dry matter fraction m_d and the temperature dependent saline water dielectric constant ϵ_{sw}. This constant was determined with a dielectric model of sea water [13]. For the salinity, we used a constant value of $0.5\,\%$. The quotient of the the dried leaf mass and the fresh leaf mass m_d was determined to a value of approx. 0.4. For our model opacity τ_{mod}, we keep all of the above inputs fixed with the exception of the canopy temperature T_c.

C. Measurement and modeling examples

Time series of the measured canopy opacity τ_{me} and τ_{mod} as well as of the canopy infrared temperature are shown in Figure 3 during an almost rainless period of 4 days.

IV. Results and Discussion

In the upper panel of Figure 3 we see that our opacity measurements and the modeled opacities are anti-correlated. Therefore we conclude that the measured opacity τ_{me} must be expressed as a sum of different opacity contributions:

$$\tau_{\mathrm{me}} = \tau_{\mathrm{diu}} + \tau_{\mathrm{wet}} + \tau_{\mathrm{mod}} \qquad (4)$$

with τ_{diu} being the diurnal contribution and τ_{wet} being the contribution coming from water on the leaves. In this equation, τ_{mod} only accounts for opacity changes due to the change in temperature of the canopy. The difference $\tau_{\mathrm{me}} - \tau_{\mathrm{mod}}$ during a rain- and dewfree period ($\tau_{\mathrm{wet}} = 0$) leads to the diurnal

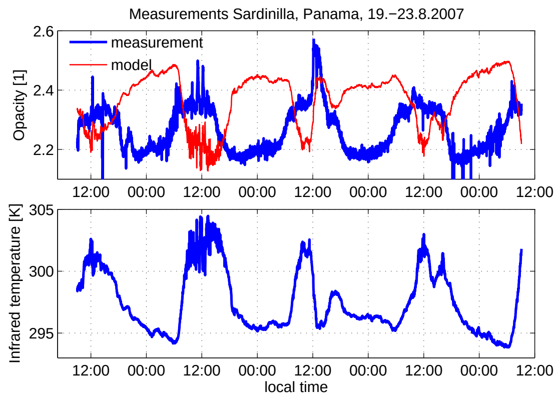

Fig. 3. Time series of modeled and measured opacity (upper panel) and the canopy infrared temperature (lower panel). The shown period was dry with the exception of a weak rain shower ($5\,\mathrm{mm}$ of rain) around 12 o'clock at the third day.

contribution, which is plotted in in Figure 4 together with PAR, VPD and the CO_2 and water vapor fluxes for the same period as in Figure 3. It is obvious that there is a strong correlation between the diurnal opacity τ_{diu} and the other plotted variables.

VPD and PAR are proxies for the flow of sap in the tree. Since τ_{diu} has to originate from one or several of the input parameters of the opacity model that were held constant (d, m_d, salinity), we conclude that sap flow induces changes in one or several of these parameters.

If we want to study τ_{wet}, we have to model τ_{diu} with one of the variables of Figure 4. We achieve the best fit with the

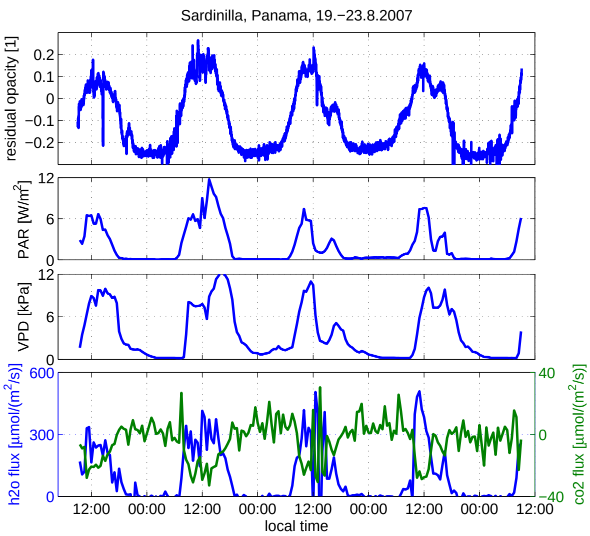

Fig. 4. Time series of the diurnal opacity contribution τ_{diu}, VPD, PAR and the eddy fluxes for the same time period as in Figure 3

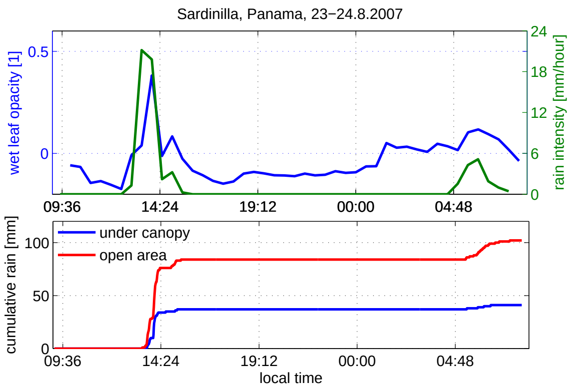

Fig. 5. Upper panel: τ_{wet} (blue curve) and the difference between the open area rain intensity and the rain intensity under the canopy with a time resolution of 30 min (green curve). Lower panel: The cumulative rain sum from the two tipping buckets with a one minute time resolution.

following expression:

$$\tau_{\mathrm{diu}} = 0.055 + 0.4 \cdot \mathrm{PAR} \cdot \mathrm{e}^{(-0.7 \cdot \mathrm{PAR} + 0.002)} - 0.3 \qquad (5)$$

This Equation together with Eq. 4 allows us to calculate τ_{wet} as a function of PAR, τ_{me} and τ_{mod}. In the upper panel of Figure 5, τ_{wet} is plotted together with the difference between the cumulative rain sum of the two tipping buckets divided by the 30 min time bin for a period with two rain events. We see a strong resemblance between the two curves, but the increase of the microwave signal during the night is not reflected in the green curve. We assume that this increase is induced by dew deposition on the leaves during the night.

V. Conclusion

We have shown some evidence that the observed diurnal cycle in the residual opacity can be explained with dielectric changes in the leaves induced by sap flow. We have also shown that water deposited on the leaves has a strong influence on the canopy opacity. If we are able to accurately model the diurnal opacity cycle, we can calculate the opacity change due to leaf wetness. This method can possibly be used for dew deposition, evapotranspiration and rain interception studies.

Acknowledgment

Since this project was based on a private initiative, I am very grateful for the financial support I received from the following Swiss institutions: Prof. Heinrich Greinacher Foundation; Travel grants commission and the Remote sensing commission of the Swiss Academy of Sciences SCNAT; Institute of Plant Sciences, Federal Institute of Technology; Institute of Applied Physics, University of Bern.

Further, I am also very appreciative to logistics support provided by the Smithsonian Tropical Research Institute, Panama and to Prof. Catherine Potvin from the McGill University, Canada, who allowed me to conduct this project on her research plantation. I would like to thank the Institute of Geography of the University of Bern that lent me the hemispherical camera and last but not least José and Iliana Monteza-Cabrera with family who shared their home with me and made my stay very comfortable.

References

[1] A. A. Chukhlantsev, *Microwave Radiometry of Vegetation Canopies*. 3300 AA Dordrecht, The Netherlands: Springer, 2006.

[2] K. C. McDonald, R. Zimmermann, and J. S. Kimball, "Diurnal and spatial variation of xylem dielectric constant in norway spruce (picea abies [l.] karst.) as related to microclimate, xylem sap flow, and xylem chemistry," *IEEE Trans. Geosci. Remote Sens.*, vol. 40, no. 9, pp. 2063–2082, 2002.

[3] M. Satake and H. Hanado, "Diurnal change of amazon rain forest σ^0 observed by Ku-band spaceborne radar," *IEEE Trans. Geosci. Remote Sens.*, vol. 42, no. 6, pp. 1127–1134, 2004.

[4] J. Way, J. Paris, M. Dobson, K. McDonald, F. T. Ulaby, and J. Vanderbilt, "Diurnal change in trees as observed by optical and microwave sensors: The Eos synergism study," *IEEE Trans. Geosci. Remote Sens.*, vol. 29, no. 6, pp. 817–820, 2004.

[5] W. Bouten, P. Swart, and E. D. Water, "Microwave transmission, a new tool in forest and hydrological research," *J. of Hydrology*, vol. 124, no. 1-2, pp. 119–130, 1991.

[6] M. Guglielmetti, M. Schwank, C. Mätzler, C. Oberdörster, J. Vanderborght, and H. Flühler, "Measured microwave radiative transfer properties of a deciduous forest canopy," *Remote Sens. Environ.*, vol. 109, no. 4, pp. 523–532, 2007.

[7] C. Mätzler, "Microwave transmissivity of a forest canopy: Experiments made with a beech," *Remote Sens. Environ.*, vol. 48, pp. 172–180, 1994.

[8] P. W. Rosenkranz, "Retrieval of temperature and moisture profiles from AMSU-A and AMSU-B measurements," *IEEE Trans. Geosci. Remote Sens.*, vol. 39, no. 11, pp. 2429–2435, 2001.

[9] ——, "Water vapor microwave continuum absorption: A comparison of measurements and models," *Radio Sci.*, vol. 33, pp. 919–928, 1998.

[10] U. Wegmüller, C. Mätzler, and E. G. Njoku, "Canopy opacity models," in *Passive Microwave Remote Sensing of Land-Atmosphere Interactions*, E. G. Njoku, P. Pampaloni, B. J. Choudhury, and Y. H. Kerr, Eds. Utrecht, The Netherlands: VSP, 1995, pp. 375–387.

[11] J. A. Kong, *The Theory of Electromagnetic Waves*. New York: J. Wiley & Sons, 1975.

[12] C. Mätzler, "Microwave (1 – 100 GHz) dielectric model of leaves," *IEEE Trans. Geosci. Remote Sens.*, vol. 32, no. 5, pp. 947–949, 1994.

[13] T. Meissner and F. J. Wentz, "The complex dielectirc constant of pure and sea water from microwave satellite observations," *IEEE Trans. Geosci. Remote Sens.*, vol. 42, no. 9, pp. 1836–1849, 2004.